

Chlorophyll anomalies along the critical latitude at 30°N in the NE Pacific

Cara Wilson¹

Received 25 May 2011; revised 20 June 2011; accepted 21 June 2011; published 3 August 2011.

[1] The dissipation of surface tidal energy into internal tides plays a critical role in ocean mixing. However, quantifying the spatial distribution of this energy flux, which is required for ocean and climate modeling, has been largely based on modeling efforts and there is a need for validating observations. The summer development of large blooms of chlorophyll along 30°N in the E. Pacific is presented as evidence of enhanced tidal mixing. The region near 30° is a “double” critical latitude, with a transformation of internal waves occurring at both diurnal and semidiurnal frequencies. The breakdown at the critical latitude of internal waves generated at Hawaii could provide the physical mechanism to explain these blooms. The blooms develop in a region characterized by a weak summer surface stratification, which is therefore more susceptible to mixing. **Citation:** Wilson, C. (2011), Chlorophyll anomalies along the critical latitude at 30°N in the NE Pacific, *Geophys. Res. Lett.*, 38, L15603, doi:10.1029/2011GL048210.

1. Introduction

[2] Measurements of turbulent mixing in the ocean are an order of magnitude weaker than has been calculated as needed to drive the large-scale ocean thermohaline circulation, suggesting that there must be localized areas of intensified mixing [Munk and Wunsch, 1998; Rudnick et al., 2003]. Tidal mixing, and the cascade of energy involving surface tides, internal waves (IWs), breaking IWs, and turbulence generation have been postulated to supply about half of the required energy [Rudnick et al., 2003]. Better estimates of ocean mixing and its geographical variability are needed to improve global ocean circulation and climate models [Alford and Zhao, 2007]. While there have been many modeling studies on IWs and their potential contribution to ocean mixing, observational evidence is harder to obtain [Gerkema and Shrira, 2006; MacKinnon and Winters, 2005; Simmons, 2008].

[3] One of the most prominent areas of deep-ocean tidal energy loss is the Hawaiian Ridge [Merrifield et al., 2001; Rudnick et al., 2003]. While it occupies <0.3% of the global ocean area, it is estimated to account for 2% of the global deep water tidal energy loss [Rudnick et al., 2003]. Approximately half of the energy loss at the Hawaiian Ridge is radiated away through IWs [Merrifield et al., 2001; Rudnick et al., 2003], and some have been observed to propagate as

far north as 40°N [Alford and Zhao, 2007; Dushaw et al., 1995] and the Aleutian Islands [Zhao and Alford, 2009]. Results from the Hawaii Ocean Mixing Experiment have reduced the uncertainties in the tidal energy budget around Hawaii, but there are still questions about where and how all of the energy is dissipated [Pinkel and Rudnick, 2006], and there are probably hot spots of turbulence that have not been observed [Klymak et al., 2006].

[4] Latitude impacts the behavior of IWs. The term “critical latitude” has been used in reference to two different dynamics. At the inertial latitude, λ_I , the tidal frequency, ω , equals the inertial frequency, f [Furevik and Foldvik, 1996; Robertson, 2001]. This latitude is also called the ‘turning latitude’ as internal tides can not propagate poleward of it, and must travel equatorward towards lower f . Diurnal tidal components have λ_I near 30°, whereas for semi-diurnal tidal components, which generally predominate, the λ_I occur at higher latitudes, poleward of 70°. The major tidal components and their λ_I are summarized in Table 1.

[5] The term “critical latitude” has also been used to refer to the latitude where the tidal frequency is twice the local inertial frequency [Alford et al., 2007; MacKinnon and Winters, 2005]. At this latitude there is potential for enhanced mixing through parametric subharmonic instability (PSI) [MacKinnon and Winters, 2004]. Here this latitude will be referred to as λ_{PSI} , and these values for the tidal components are also given in Table 1. Diurnal tidal components have λ_{PSI} near 15°, and for semi-diurnal tidal components it is near 30°. The region near 30° is a “double” critical latitude, with potential energy loss occurring at both diurnal and semidiurnal frequencies (Table 1). In the rest of this paper the term “critical latitude” will refer to ~30°, where both the semi-diurnal λ_{PSI} and the diurnal λ_I occur. Both semi-diurnal (M_2) and diurnal (K_1) tidal components are considered.

[6] Modeling studies have indicated that enhanced mixing should be occurring at both the λ_{PSI} and the λ_I , but there is a general paucity of supporting observational data [Gerkema and Shrira, 2006; Simmons, 2008]. Here evidence of enhanced mixing at the critical latitude (30°N) in the N. Pacific, is introduced in the form of summertime chlorophyll *a* (chl) blooms which have consistently been observed by satellite data (Figure 1) in this area [Dore et al., 2008; Wilson and Qiu, 2008]. So far there has not been an adequate physical mechanism to explain the formation of these features. While Finite Size Lyapunov Exponents have been used to explain the evolution of these features, the specific mechanisms of nutrient injection remain unclear [Calil et al., 2011; Calil and Richards, 2010]. The idea that IWs are generating a biological response in this region is not new. Observations of enhanced summer production at the CLIMAX site (see Figure 1) in the late 1960s led McGowan

¹NOAA, Southwest Fisheries Science Center, Environmental Research Division, Pacific Grove, California, USA.

Table 1. Frequencies of the Eight Primary Tidal Components, Their Relative Contribution, and Their Critical Latitudes^a

Constituent	Period (Hours)	Normalized Amplitude Function ^b	Critical Latitude $\lambda_l, \omega = f$	PSI Critical Latitude $\lambda_{PSI}, \omega = 2f$
M ₂	12.42	1.00	74.5°	28.8°
S ₂	12.00	0.47	85.8°	29.9°
N ₂	12.66	0.23	71.0°	28.2°
K ₂	11.97	0.12	88.8°	30.0°
K ₁	23.93	0.59	30.0°	14.5°
O ₁	25.82	0.42	27.6°	13.4°
P ₁	24.07	0.19	29.8°	14.4°
Q ₁	26.87	0.08	26.5°	12.9°

^aCritical latitudes near 30° are bolded.

^bFrom *Simmons et al.* [2004].

and *Hayward* [1978] to suggest that breaking IWs were creating enhanced mixing in this region.

2. Data

[7] Monthly and weekly composites of satellite chl data from SeaWiFS from 1997–2006 and from MODIS from 2007–2010 were analyzed. ARGO float data from 2006–2010, and nutrient data from the World Ocean Atlas 2009 [*Garcia et al.*, 2010] were used to examine hydrographic conditions within the bloom region. The satellite and ARGO data were acquired from the ERDDAP server at NOAA/SWFSC/ERD, and the nutrient data from the LDEO/IRI data library.

3. The Bloom Region

[8] Chl blooms near 30°N in the NE Pacific are consistent events in the late summer. These features have been mostly unsampled and it is not clear what physical dynamics cause them [*Dore et al.*, 2008; *Villareal et al.*, 2011; *Wilson and Qiu*, 2008; *Wilson et al.*, 2008]. While there is interannual variability in the location of the chl blooms, and there have been some years when they do not develop [*Wilson and Qiu*, 2008], they generally develop northeast of the Hawaiian Ridge, in a region bounded by 130°–160°W and 29°–34°N

(Figure 1). With the exception of one spring bloom in 2010, they have never developed west of the Hawaiian Ridge [*Calil et al.*, 2011]. Their location has more longitudinal variability than latitudinal, and the longitudinal variation has a bi-modal distribution; they tend to have either an eastern location centered near 138°W, or a western location near 152°W. This distribution can be seen more clearly in Figure 2, which shows the specific surface initiation point of individual blooms, determined from analysis of weekly chl images.

[9] The dominant phytoplankton associated with the chl blooms are diatoms with nitrogen-fixing endosymbionts [*Dore et al.*, 2008; *Villareal et al.*, 2011; *Wilson et al.*, 2008], whose growth is limited by phosphate, silicate or iron. *Dore et al.* [2008] postulate that the chl blooms are controlled mainly by phosphate supply, and that their development in the eastern part of the NE Pacific is due to the shallower phosphacline there. *Calil et al.* [2011] argue that the western 2010 bloom was triggered in part by anomalous dust deposition alleviating iron limitation.

[10] Here it is hypothesized that enhanced mixing at the critical latitude, caused by the breakdown of IWs generated at the Hawaiian Ridge, provides the nutrient injection that stimulates the observed chl blooms. This mechanism would also explain why the blooms predominately develop east of Hawaii. The waves propagate roughly perpendicular to the ridge axis, so they travel either northeast or southwest. The waves traveling southwest would not encounter the critical latitude at 30°N. Furthermore the bi-modal distribution pattern of the blooms' location can also be related to the pattern of IW generation at the Hawaiian Ridge. IW generation does not occur uniformly along the Hawaiian Ridge, rather there are certain “hot spots” where the energy fluxes are stronger [*Merrifield et al.*, 2001; *Rudnick et al.*, 2003; *Zhao et al.*, 2010]. These occur at French Frigate Shoals (FFS, 166.1°W), Nihoa Island (NI, 162°W) and the Kauai Channel (KC, 158.8°W) and are indicated on Figure 2, along with the northeast M₂ energy fluxes from the PEZHAT numerical model (courtesy of E. Zaron). The two most northerly pathways from FFS and NI cross the critical latitude near 160°W, slightly west of the bloom region, while a northeast path out of FFS crosses the critical latitude in the western region of where the blooms develop. Fluxes from KC are more easterly, and while the model domain does

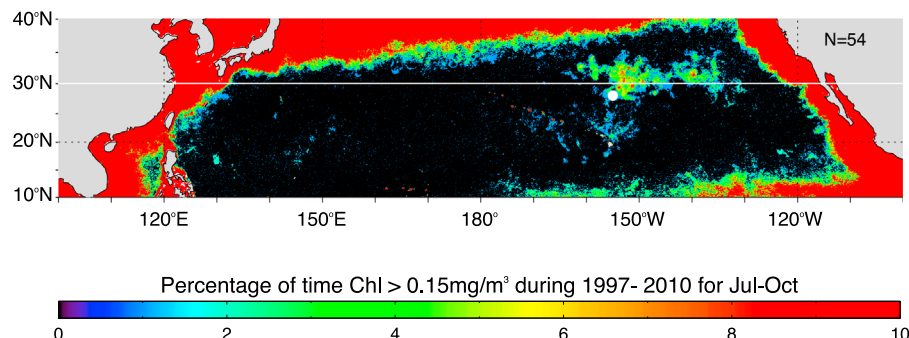


Figure 1. The percentage of time that chl is above 0.15 mg/m³ during Jul–Oct of 1997–2010 in the N. Pacific (n = 54). Monthly data, for July through October, from SeaWiFS for 1997–2006, and from MODIS for 2007–2010 were used. The summer chl blooms develop between 130°–160°W near the K₁ λ_c , and the M₂ λ_{PSI} , as indicated by the white line at 30°N. The white dot is the location of the CLIMAX station. The bloom area (defined as 25°–35°N, 150°–130°W) has a minimum number of 36 datapoints, and is mostly outside of the region of persistent cloudiness that occurs between 120°–140°W, and 20°–30°N.

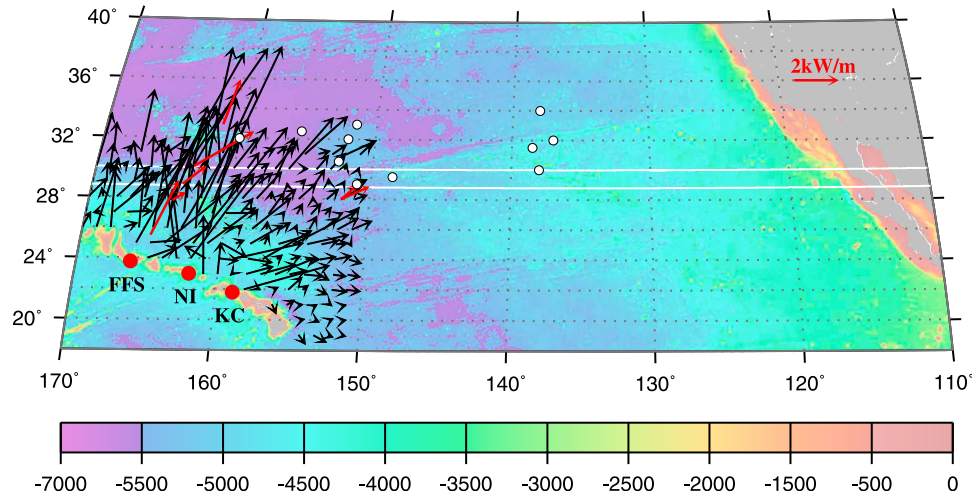


Figure 2. Bathymetry map of the NE Pacific bloom region, showing the locations of the different surface initiation points of the chl blooms (white dots), at the eastern and western edges of the Murray Fracture Zone. The locations of the three “hotspots” of internal wave generation along the Hawaiian Ridge are also shown (red dots), along with the northeast M₂ energy fluxes from the PEZHAT numerical model (E. Zaron, personal communication, 2011). The red arrows indicate the M₂ energy fluxes calculated from mooring data of Alford and Zhao [2007] and Zhao et al. [2010].

not extend that far, extrapolation of the flux directions has them crossing the critical latitude near 140°W, in the eastern lobe of the bloom region. Energy fluxes determined from mooring data from 28°N, 152°W [Alford and Zhao, 2007] are slightly larger than the model estimates but in the same direction (Figure 2). Altimetric estimates of the internal tide are negligible in the eastern portion of the bloom region [Ray and Cartwright, 2001; Zhao and Alford, 2009], however, they can not resolve signals that have been modified from interactions with varying stratification or eddy fields [Chiswell, 2006; Rainville and Pinkel, 2006].

[11] As mentioned previously there are processes near 30° that impact both semi-diurnal and diurnal tidal components. Both are considered here because Hawaii lies near the semi-diurnal amphidromic point [Ray, 1999], and as a result the semi-diurnal tidal amplitude does not dominate here as much as in other regions of the ocean. It is interesting to note that the blooms actually develop within the semi-diurnal amphidromic point (see auxiliary material).¹ The amplitudes of the M₂ and K₁ tidal components at Hawaii are 20 cm and 15 cm respectively [Ray, 1999]. However, it appears that the semi-diurnal baroclinic waves are generated more efficiently than the diurnal tides [Chiswell, 2002].

4. PSI

[12] Studies of PSI, the process where energy is transferred from the semi-diurnal M₂ internal tide to its subharmonic ½M₂, have focused on the λ_{PSI} at 28.8° [Hibiya and Nagasawa, 2004; MacKinnon and Winters, 2004, 2005]. However, this dynamic is not restricted to just the λ_{PSI} , and can occur equatorward of it. Observations and model results indicate that substantial conversion of energy from M₂ frequencies to ½M₂ occurs near Hawaii, considerably south

of the λ_{PSI} [Carter and Gregg, 2006; Xie et al., 2011]. However, at the λ_{PSI} the recipient waves are almost inertial and can't propagate further northward (see next section) and remain trapped locally [MacKinnon and Winters, 2005]. MacKinnon and Winters [2004] estimate that at the λ_{PSI} nearly 80% of the tidal energy is dissipated locally, resulting in “mixing hotspots” at 28.8°.

5. Inertial Latitude

[13] Under linear wave theory, when IWs are at their inertial latitude they can no longer propagate poleward and are reflected towards the equator. However, recent work taking into account “non-traditional effects”, i.e., the horizontal component of the earth's rotation, shows that waves can penetrate past their inertial latitude [Gerkema and Shrira, 2005]. Shrira and Townsend [2010] describe a phenomenon called singular focusing where IWs continue past the λ_{I} in narrow waveguides bounded by local minima in the buoyancy frequency, N². The waves do not propagate indefinitely, there is a “absorption latitude”, which can be several degrees poleward of the λ_{I} depending on local stratification. IWs accumulate at the “absorption latitude,” and the simultaneous increase in wave amplitude and decrease in vertical scale leads to increased mixing within these N² minima waveguides [Gerkema and Shrira, 2005; Shrira and Townsend, 2010].

[14] To see where these waveguides occur within the bloom region, sections of the buoyancy frequency along 30°N, calculated from ARGO float data, are shown in Figure 3. Throughout the year the subsurface N² maximum is at 50–100 m depth in the western part of the section near 180°W and gradually deepens to 200–250 m depth at 130°W. In the summertime (Figure 3b) a layer of high N² develops near 50 m depth. It is stronger in the west, but extends across the entire section, creating a subsurface N² minimum at 50–150 m depth between 130°–150°W, the same region where the chl blooms develop. The depth of the subsurface N² minimum is coincident with the phosphacline, as indicated

¹Auxiliary materials are available in the HTML. doi:10.1029/2011GL048210.

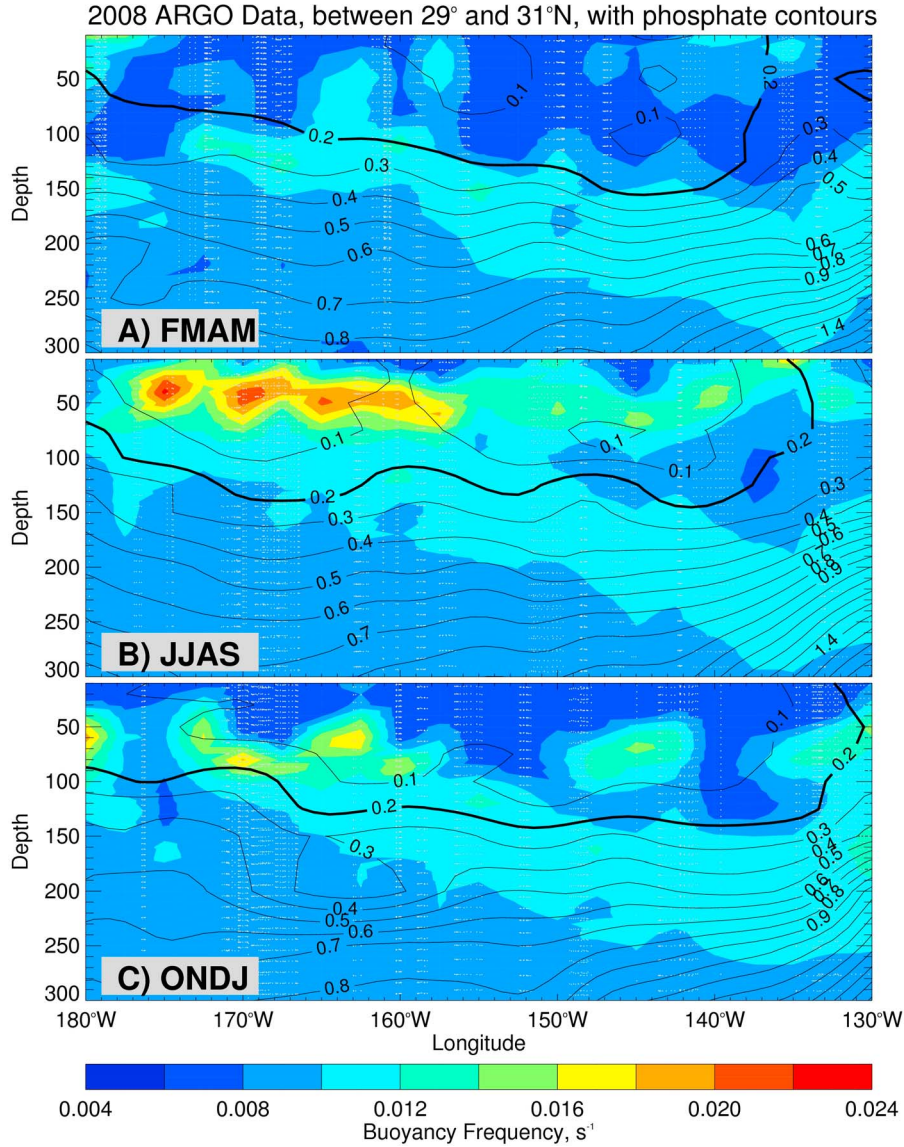


Figure 3. Sections of N^2 , the buoyancy frequency, along 30°N computed from ARGO float data between $29^\circ\text{--}31^\circ\text{N}$ and $180^\circ\text{--}130^\circ\text{W}$ from (a) Feb–May 2008, (b) Jun–Sep 2008 and (c) Oct 2008–Jan 2009. The overlaid contours are the climatological phosphate values for that season from the World Ocean Atlas 2009 [Garcia et al., 2010]. The small gray dots indicate the locations of the ARGO data. While only data from 2008 is shown, ARGO data from 2005–2010 were examined, and all other years had the same seasonal pattern.

by the contours of phosphate on Figure 3, so enhanced mixing within the N^2 minimum waveguide would deliver nutrients into the surface layer. West of this region there is no subsurface N^2 minimum, and with virtually no N^2 minimum at the surface, mixing induced by singular focusing will get focused in the N^2 minimum in the deep ocean. Outside of the bloom season (Figures 3a and 3c) mixing will be focused in the N^2 minimum at the surface or at depth. However the surface N^2 minimum does not intersect with the phosphacline and therefore mixing will not lead to an upward nutrient flux. The summer stratification pattern (Figure 3b) explains why blooms are not observed west of $\sim 150^\circ\text{W}$, despite the concentrated tidal fluxes that arrive there (Figure 2). The fall stratification pattern shows some bimodality in the buoyancy frequency around 140°W and

155°W (Figure 3c) that is similar to the bloom distribution (Figure 1).

6. Other Factors

[15] The chl blooms often develop around the periphery of anticyclonic eddies [Calil and Richards, 2010; Wilson and Qiu, 2008]. Yet paradoxically, the region of the Pacific where the blooms develop is one with extremely weak eddy kinetic energy (EKE) [Calil and Richards, 2010; Wilson and Qiu, 2008]. The EKE drops by an order of magnitude, from values $>300 \text{ cm}^2 \text{ s}^{-2}$ west of the dateline to $<30 \text{ cm}^2 \text{ s}^{-2}$ in the bloom region [Ducet et al., 2000]. If the blooms were generated purely by eddy dynamics they should be concentrated in the western N. Pacific, where they are conspicuously absent, not in the eastern N. Pacific where the EKE is

low. This paradox is repeated on a local level, as the eddies that the blooms develop around are generally not the strongest eddies in the area [Wilson and Qiu, 2008]. Calil and Richards [2010] demonstrate that the 30°N chl anomalies are located in regions of large stretching of the background flow field. However, they note that while the horizontal stirring resulting from the flow field controls the evolution of the chl distribution, the local vertical nutrient injection is a separate process.

[16] In discussing the difficulty of finding observational evidence for enhanced mixing associated with the λ_{PSI} , Simmons [2008] suggests that eddy dynamics, which are not included in most internal wave models, could have an important impact, specifically that a strong eddy field could smear out the effects of PSI. This offers an additional explanation why the blooms develop along the critical latitude in the eastern, but not the western, N. Pacific. Namely, the strong EKE field in the western N. Pacific dampens out the PSI effects, while the weak EKE in the eastern N. Pacific allows these processes to be better manifested.

[17] A factor of two difference in the amount of tidal energy conversion occurring at KC was observed from just a six-month deployment [Zilberman et al., 2011]. It's possible that the location of the bloom every year could be revealing interannual differences in the strength of the tidal fluxes generated at the Hawaiian Ridge. However, before arriving at the critical latitude both the magnitude and direction of the tidal fluxes could have been modified from interactions with the mesoscale current field, varying stratification and other IWs [Alford et al., 2007; Chavanne et al., 2010; Rainville and Pinkel, 2006], which will complicate the potential relationship between the strength of IW generation at the ridge and bloom development at the critical latitude.

[18] Clearly the Hawaiian Ridge is not the only hot spot in the ocean where IWs are being generated, and it is logical to wonder if similar bloom features are observed elsewhere. The trick is to find an area where (1) the IW's beams are intense enough to make a substantial impact at the critical latitude, and (2) the environment is simple enough so that a clear biological signal can be identified. Given the general dominance of the semi-diurnal component of tides (see Table 1) most studies have focused on the semi-diurnal λ_I at high latitudes [Makinson et al., 2006; Robertson, 2001], and enhanced productivity attributed to the λ_I has been observed in the Barents Sea [Furevik and Foldvik, 1996]. However, detecting anomalous chl signals will be challenging at the high latitude λ_I given the more complicated biological dynamics there. The Tuamoto Archipelago ($\sim 18^{\circ}\text{S}$, 145°W) in the S. Pacific is a region of IW generation [Simmons et al., 2004], but no chl anomalies are observed along 30°S where the waves would cross the critical latitude [Wilson and Qiu, 2008]. However, the behavior of IWs can vary at different generation points. The single high ridge at Hawaii generates waves that propagate long distances, but at small-scale topographical features, such as the Tuamoto Archipelago, most of the energy probably goes into modes that do not propagate far before dissipating [Nycander, 2005] and so would not reach 30°S . Chl anomalies have been observed in the S. Pacific around New Caledonia and Vanuatu [Wilson and Qiu, 2008], another region of IW generation [Simmons et al., 2004]. The dynamics in this area are complicated by the topography and the multitude of islands, such that there are

numerous factors that could be driving the chl variability in this region [Wilson and Qiu, 2008].

7. Summary

[19] Satellite chl data has led to the discovery of substantial late summer chl blooms in the oligotrophic NE pacific gyre. While we have a basic understanding of the phytoplankton community involved [Dore et al., 2008; Villareal et al., 2011; Wilson et al., 2008], the physical stimulus for these blooms has remained more elusive. Their consistent development in the NE Pacific, rarely occurring west of Hawaii, indicates that basin-scale mechanisms are responsible. The Hawaiian Ridge is a "hotspot" for IW generation, with the waves propagating roughly normal to the ridge, i.e., in a northeast and southwest direction. The breakdown of these IWs at the critical latitude can explain the consistent location of these features in the NE Pacific. The location of the bloom every year could be revealing interannual differences in the strength of the tidal fluxes from the different generation points. Basin-scale changes in EKE, stratification and nutrient distributions [Dore et al., 2008] are all probably contributing factors to the development of the blooms in the eastern NE Pacific. Future modeling studies of IWs should try to simulate the biological features observed by satellite data.

[20] **Acknowledgments.** Thanks to the Ocean Color Data Processing group at NASA/GSFC for their generation and maintenance of climate-quality ocean color data records. The ARGO data were collected and made freely available by the International Argo Program and the national programs that contribute to it. Thanks to Harper Simmons, Jonas Nycander and Ed Zaron for entertaining my questions and for their feedback, to Adrian Burd for suggesting that the critical latitude might play a role in the initiation of the blooms, and to Andrew Leising and Steven Bograd for their comments on an earlier version of this paper. Comments from two anonymous reviewers improved this paper.

[21] The Editor thanks two anonymous reviewers for their assistance in evaluating this paper.

References

- Alford, M. H., and Z. Zhao (2007), Global patterns of low-mode internal wave propagation. Part I: Energy and energy flux, *J. Phys. Oceanogr.*, **37**, 1829–1848, doi:10.1175/JPO3085.1.
- Alford, M. H., J. A. MacKinnon, Z. Zhao, R. Pinkel, J. Klymak, and T. Peacock (2007), Internal waves across the Pacific, *Geophys. Res. Lett.*, **34**, L24601, doi:10.1029/2007GL031566.
- Calil, P. H. R., and K. J. Richards (2010), Transient upwelling hot spots in the oligotrophic North Pacific, *J. Geophys. Res.*, **115**, C02003, doi:10.1029/2009JC005360.
- Calil, P. H. R., S. C. Doney, K. Yumimoto, K. Eguchi, and T. Takemura (2011), Episodic upwelling and dust deposition as bloom triggers in low-nutrient, low-chlorophyll regions, *J. Geophys. Res.*, **116**, C06030, doi:10.1029/2010JC006704.
- Carter, G. S., and M. C. Gregg (2006), Persistent near-diurnal internal waves observed above site of M_2 barotropic-to-baroclinic conversion, *J. Phys. Oceanogr.*, **36**, 1136–1147, doi:10.1175/JPO2884.1.
- Chavanne, C., P. Flament, G. Carter, M. Merrifield, D. Luther, E. Zaron, and K.-W. Gurgel (2010), The surface expression of semidiurnal internal tides near a strong source at Hawaii. Part I: Observations and numerical predictions, *J. Phys. Oceanogr.*, **40**, 1155–1179, doi:10.1175/2010JPO4222.1.
- Chiswell, S. M. (2002), Energy levels, phase, and amplitude modulation of the baroclinic tide off Hawaii, *J. Phys. Oceanogr.*, **32**, 2640–2651, doi:10.1175/1520-0485-32.9.2640.
- Chiswell, S. M. (2006), Altimeter and current meter observations of internal tides: Do they agree?, *J. Phys. Oceanogr.*, **36**, 1860–1872, doi:10.1175/JPO2944.1.
- Dore, J. E., R. M. Letelier, M. J. Church, and D. M. Karl (2008), Summer phytoplankton blooms in the oligotrophic North Pacific subtropical gyre:

- Historical perspective and recent observations, *Prog. Oceanogr.*, 76, 2–38, doi:10.1016/j.pocean.2007.10.002.
- Ducet, N., P. Y. Le Traon, and G. Reverdin (2000), Global high-resolution mapping of ocean circulation from TOPEX/Poseidon and ERS-1 and-2, *J. Geophys. Res.*, 105, 19,477–19,498, doi:10.1029/2000JC900063.
- Dushaw, B. D., B. D. Cornuelle, P. F. Worcester, B. M. Howe, and D. S. Luther (1995), Barotropic and baroclinic tides in the central North Pacific Ocean determined from long-range reciprocal acoustic transmissions, *J. Phys. Oceanogr.*, 25, 631–647, doi:10.1175/1520-0485(1995)025<0631:BABTT>2.0.CO;2.
- Furevik, T., and A. Foldvik (1996), Stability at M_2 critical latitude in the Barents Sea, *J. Geophys. Res.*, 101, 8823–8837, doi:10.1029/96JC00081.
- Garcia, H. E., R. A. Locarnini, T. P. Boyer, and J. I. Antonov (2010), *World Ocean Atlas 2009*, vol. 4, *Nutrients (Phosphate, Nitrate, and Silicate)*, NOAA *Atlas NESDIS*, vol. 71, edited by S. Levitus, 398 pp., NOAA, Silver Spring, Md.
- Gerkema, T., and V. I. Shrira (2005), Near-inertial waves in the ocean: Beyond the ‘traditional approximation,’ *J. Fluid Mech.*, 529, 195–219, doi:10.1017/S0022112005003411.
- Gerkema, T., and V. I. Shrira (2006), Non-traditional reflection of internal waves from a sloping bottom, and the likelihood of critical reflection, *Geophys. Res. Lett.*, 33, L06611, doi:10.1029/2005GL025627.
- Hibiya, T., and M. Nagasawa (2004), Latitudinal dependence of diapycnal diffusivity in the thermocline estimated using a finescale parameterization, *Geophys. Res. Lett.*, 31, L01301, doi:10.1029/2003GL017998.
- Klymak, J. M., J. N. Moum, J. D. Nash, E. Kunze, J. B. Girton, G. S. Carter, C. M. Lee, T. B. Sanford, and M. C. Gregg (2006), An estimate of tidal energy lost to turbulence at the Hawaiian Ridge, *J. Phys. Oceanogr.*, 36, 1148–1164, doi:10.1175/JPO2885.1.
- MacKinnon, J. A., and K. B. Winters (2004), Tidal mixing hotspots governed by rapid parametric subharmonic instability, *J. Phys. Oceanogr.*, 34, 1–9.
- MacKinnon, J. A., and K. B. Winters (2005), Subtropical catastrophe: Significant loss of low-mode tidal energy at 28.9° , *Geophys. Res. Lett.*, 32, L15605, doi:10.1029/2005GL023376.
- Makinson, K., M. Schröder, and S. Østerhus (2006), Effect of critical latitude and seasonal stratification on tidal current profiles along Ronne Ice Front, Antarctica, *J. Geophys. Res.*, 111, C03022, doi:10.1029/2005JC003062.
- McGowan, J. A., and T. L. Hayward (1978), Mixing and oceanic productivity, *Deep Sea Res.*, 25, 771–793, doi:10.1016/0146-6291(78)90023-1.
- Merrifield, M. A., P. E. Holloway, and T. M. S. Johnston (2001), The generation of internal tides at the Hawaiian Ridge, *Geophys. Res. Lett.*, 28, 559–562, doi:10.1029/2000GL011749.
- Munk, W., and C. Wunsch (1998), Abyssal recipes II: Energetics of tidal and wind mixing, *Deep Sea Res., Part I*, 45, 1977–2010, doi:10.1016/S0967-0637(98)00070-3.
- Nycander, J. (2005), Generation of internal waves in the deep ocean by tides, *J. Geophys. Res.*, 110, C10028, doi:10.1029/2004JC002487.
- Pinkel, R., and D. Rudnick (2006), Editorial, *J. Phys. Oceanogr.*, 36, 965–966, doi:10.1175/JPO9022.1.
- Rainville, L., and R. Pinkel (2006), Propagation of low-mode internal waves through the ocean, *J. Phys. Oceanogr.*, 36, 1220–1236, doi:10.1175/JPO2889.1.
- Ray, R. D. (1999), A global ocean tide model from TOPEX/POSEIDON Altimetry: GOT99.2, *NASA Tech. Memo. NASA/TM-1999-209478*, 58 pp., NASA Goddard Space Flight Cent., Greenbelt, Md.
- Ray, R. D., and D. E. Cartwright (2001), Estimates of internal tide energy fluxes from Topex/Poseidon altimetry: Central North Pacific, *Geophys. Res. Lett.*, 28, 1259–1262, doi:10.1029/2000GL012447.
- Robertson, R. (2001), Internal tides and baroclinicity in the southern Weddell Sea: 2. Effects of the critical latitude and stratification, *J. Geophys. Res.*, 106, 27,017–27,034, doi:10.1029/2000JC000476.
- Rudnick, D. L., et al. (2003), From tides to mixing along the Hawaiian ridge, *Science*, 301, 355–357, doi:10.1126/science.1085837.
- Shrira, V. A., and W. A. Townsend (2010), Inertia-gravity waves beyond the inertial latitude. Part 1. Inviscid singular forcing, *J. Fluid Mech.*, 664, 478–509, doi:10.1017/S0022112010003812.
- Simmons, H. L. (2008), Spectral modification and geographic redistribution of the semi-diurnal internal tide, *Ocean Modell.*, 21, 126–138.
- Simmons, H. L., R. W. Hallberg, and B. K. Arbic (2004), Internal wave generation in a global baroclinic tide model, *Deep Sea Res., Part II*, 51, 3043–3068, doi:10.1016/j.dsr2.2004.09.015.
- Villareal, T. A., L. Adornato, C. Wilson, and C. A. Schoenbaechler (2011), Summer blooms of diatom-diazotroph assemblages and surface chlorophyll in the North Pacific gyre: A disconnect, *J. Geophys. Res.*, 116, C03001, doi:10.1029/2010JC006268.
- Wilson, C., and X. Qiu (2008), Global distribution of summer chlorophyll blooms in the oligotrophic gyres, *Prog. Oceanogr.*, 78, 107–134, doi:10.1016/j.pocean.2008.05.002.
- Wilson, C., T. A. Villareal, N. Maximenko, S. J. Bograd, J. P. Montoya, and C. A. Schoenbaechler (2008), Biological and physical forcings of late summer chlorophyll blooms at 30°N in the oligotrophic Pacific, *J. Mar. Syst.*, 69, 164–176, doi:10.1016/j.jmarsys.2005.09.018.
- Xie, X.-H., X.-D. Shang, H. van Haren, G.-Y. Chen, and Y.-Z. Zhang (2011), Observations of parametric subharmonic instability-induced near-inertial waves equatorward of the critical diurnal latitude, *Geophys. Res. Lett.*, 38, L05603, doi:10.1029/2010GL046521.
- Zhao, Z., and M. H. Alford (2009), New altimetric estimates of mode-1 M_2 internal tides in the central North Pacific Ocean, *J. Phys. Oceanogr.*, 39, 1669–1684, doi:10.1175/2009JPO3922.1.
- Zhao, Z., M. H. Alford, J. A. MacKinnon, and R. Pinkel (2010), Long-range propagation of the semidiurnal internal tide from the Hawaiian Ridge, *J. Phys. Oceanogr.*, 40, 713–736, doi:10.1175/2009JPO4207.1.
- Zilberman, N. V., M. A. Merrifield, G. S. Carter, D. S. Luther, M. D. Levine, and T. J. Boyd (2011), Incoherent nature of M_2 internal tides at the Hawaiian Ridge, *J. Phys. Oceanogr.*, doi:10.1175/JPO-D-10-05009.1, in press.

C. Wilson, NOAA, Southwest Fisheries Science Center, Environmental Research Division, 1352 Lighthouse Ave., Pacific Grove, CA 93950, USA. (cara.wilson@noaa.gov)